Research on Aerial View Point Planning of Drone based on Multi-View

Zhu Yan-yan Shi Yun[1]

[1]West Anhui University, Lu'an, Anhui, 237012, China

710667612@qq.com

Abstract. For multi-view viewpoint planning research, Firstly, using the UAV aerial multi-view image, the viewpoint view is first to establish a candidate view area according to the shooting distance. Secondly, the sub-viewpoint set is filtered and the view points are complemented by the region where the candidate view cannot be photographed, so that the three-dimensional reconstruction data has better integrity. Thirdly, the influence of camera incident angle on image pixel error is analyzed, and the corresponding 3D model is established. Finally, the stereoscopic overlap is used to perform viewpoint screening under the premise of ensuring image quality and shooting coverage. The experimental results show that the proposed viewpoint planning method has high coverage and the reconstruction accuracy is below 0.1% of the target size.

1. Introduction

Multi-view 3D reconstruction has the advantages of simple shooting and high measurement accuracy. It is widely used in reverse engineering, virtual reality, online detection and other occasions. For the 3D reconstruction of outdoor scenes, there are traditional measurement methods such as laser scanning and laser radar, but it is difficult to obtain complete measurement data due to measurement limitations. In this paper, the multi-rotor UAV is equipped with four monocular cameras for omnidirectional shooting of outdoor objects, and a more complete three-dimensional model can be obtained through multiple views. In order to improve the reconstruction accuracy, it is necessary to plan the viewpoint of the aerial photography process of the drone.

Viewpoint planning is a non-deterministic issue and a key technology in 3D reconstruction. In [1-3] has applications in target recognition and tracking, surface defect extraction, robot vision and other occasions. In [4] summarizes the camera viewpoint planning research. In [5], based on the principle of cross ratio invariance, the transfer relationship between image pixel error and 3D object point error is established, and the multi-view 3D reconstruction accuracy is improved. The implementation method of the motion mechanism is given in [6], and the accuracy of 3D reconstruction is improved based on the reconstruction accuracy estimation function. In [7], based on the known rough three-dimensional model of the measured object, the viewpoint is arranged in the model and then expanded. In [8] studied the extraction of key frames and 3D

reconstruction in images, but did not discuss the viewpoint planning problem.

In order to obtain a complete, high-quality image, the accuracy of the three-dimensional reconstruction is high. In this paper, aiming at the aerial vision point planning problem of UAV, by analyzing the parameter control in the aerial photography of UAV, based on the rough 3D model, the candidate viewpoint is first set and then the viewpoint planning is performed according to the constraint, thus ensuring the accuracy of 3D reconstruction.

2. Parameter Control of Camera Pose

The viewpoint represents six degrees of freedom in the camera pose in space, and its viewpoint pose can be expressed as $\boldsymbol{V}=[x_v\ y_v\ z_v\ \alpha_v\ \beta_v\ \gamma_v]^T$.

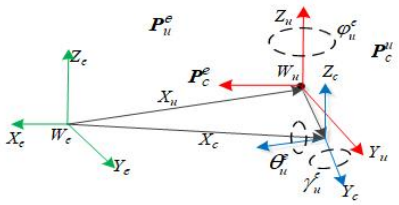

Figure 1. Relative pose of the earth, drone, camera.

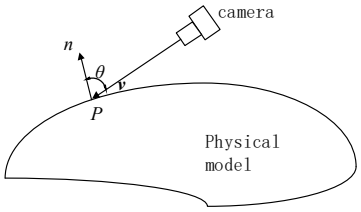

Figure 2. Schematic diagram of the viewing angle constraint.

Figure 1 shows the relative pose of the Earth, drone, and camera. The multi-rotor drone achieves flight control by setting $\boldsymbol{P}_u^e$. When the drone is hovering to capture an image, $\theta_u^e=\gamma_u^e=0$ is required.

In order to meet the multi-degree of freedom requirements for shooting, this paper adds a two-dimensional pan/tilt. The camera is mounted on the gimbal, and the gimbal is fixed directly below the fuselage. The pan/tilt provides changes in the camera's pitch angle θ_c^u and roll angle γ_c^u.The camera is mounted close to the center of gravity of the drone, and the direction of the main axis of the lens is consistent with the direction of the longitudinal axis of the drone. The viewpoint of the drone aerial photography can be controlled by the parameters of equation (1):

$$\boldsymbol{V}=[x_v\ \ y_v\ \ z_v\ \ \alpha_v\ \ \beta_v\ \ \gamma_v]^T=[x_u^e\ \ y_u^e\ \ z_u^e\ \ \varphi_u^e\ \ \theta_c^u\ \ \gamma_c^u]^T \tag{1}$$

3. Viewpoint Constraints

The target to be reconstructed needs to meet visibility constraints, overlap and coverage, motion platform constraints, and camera angle of incidence.

3.1. Visibility constraint

Visibility constraints include viewable angle, camera field of view, shooting distance, and occlusion.

(a)Viewable angle

P is a little on the surface of the object. $\boldsymbol{v}$ is the spindle vector of the camera. $\boldsymbol{N}$ is the normal vector at point P. θ is the angle between the two vectors. When $\theta<90^\circ$, P point is visible, as shown in figure 2.

(b) Camera field of view

The straight line OP should be in the longitudinal field of view angle α and the lateral direction β, and it is necessary to satisfy the formula (2).

$$\left.\begin{aligned} \boldsymbol{v}\cdot\boldsymbol{v}_{py}-\|\boldsymbol{v}\|\cdot\|\boldsymbol{v}_{py}\|\cos\frac{\alpha}{2}\geq 0 \\ \boldsymbol{v}\cdot\boldsymbol{v}_{px}-\|\boldsymbol{v}\|\cdot\|\boldsymbol{v}_{px}\|\cos\frac{\beta}{2}\geq 0 \end{aligned}\right\} \tag{2}$$

where $\boldsymbol{v}$ is the camera spindle vector. $\boldsymbol{v}_p=[x_p-x_o\ y_p-y_o\ z_p-z_o]^T$ is the vector of the OP. $\boldsymbol{v}_{px}$ and $\boldsymbol{v}_{py}$ denotes the projection loss of $\boldsymbol{v}_p$ in the plane transverse plane xO_pO and the longitudinal midplane yO_pO, respectively.

(c) Shooting distance

The shooting distance determines whether the feature can be recognized, and the shooting distance z from the lens to the surface of the object should satisfy the formula (3).

$$\left.\begin{aligned} z_{\min}=\frac{afd_{\max}}{ad_{\max}-af+cf} \\ z_{\max}=\frac{afd_{\min}}{ad_{\min}-af-cf} \end{aligned}\right\} \quad \left(f<d_{\min}<d_{\max}<2f\right) \tag{3}$$

Where a represents the aperture diameter of the camera, c represents the minimum acceptable resolution.

(d) Occlusion

As shown in figure 3, O is the center of the camera lens, P is the space object point, and triangle *efg* is *a* patch on the physical model. The parameter expression of the line *PO*:

$$p(t)=t\cdot P+(1-t)\cdot O\ \ (0\leq t\leq 1) \tag{4}$$

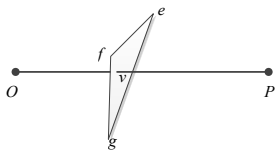

Figure 3. Blocking diagram.

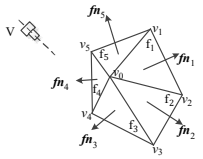

Figure 4. Supplementary view.

3.2. Overlap and coverage

The overlap between the areas captured by the camera can be calculated using equation (5).

$$\phi=S\left(C_{b1}C_{a2}\right)/S\left(C_{a1}C_{a2}\right)\times 100\% \tag{5}$$

where S represents the area of a certain area on the model.

3.3. Motion platform constraints

The camera is fixed directly below the fuselage body during aerial photography. The pan/tilt can provide angle changes of pitch and roll. The pitch angle of the viewpoint is $[-90^\circ\sim 90^\circ]$, and the roll angle is

[–45 ~ 45].

3.4. Camera angle of incidence

In [9], the shooting angle of the camera is too large, which causes the extraction accuracy of the feature points to decrease. The spacing λ on the calibration plate should satisfy the formula (6).

$$\sigma_p = \sigma_k \lambda / \|\boldsymbol{J}_k\| = \sigma_k 3\sqrt{2}\lambda / 4 \tag{6}$$

4. Viewpoint planning and screening

4.1. Candidate view area layout

The candidate viewpoints are distributed on the hemisphere with the center of the target model as the center of the sphere and the shooting distance as the radius. The shooting distance of the camera used in this paper is less than 7.5m.

4.2. Viewpoint Supplement

In order to have better integrity of the subsequent 3D reconstruction data, we use the expansion method to add visual points to the complex geometric regions that cannot be captured by candidate viewpoints, as shown in figure 4.

5. Experiment

5.1. Camera incident angle experiment and results

The screening viewpoint experiment uses a two-dimensional calibration plate that distributes 100 dot circular markers ($\lambda = 35mm$) in a range of 35 mm pitch in the 350×280 mm^2 range. In this experimental operation, the camera position is fixed, and the calibration plate attitude is changed from 0° to 75° with a minimum of 5°, and the experimental results are shown in table 1.

Table 1. Experimental Results.

Incident Angle	$\sigma_k(10^{-3})$				Error $\sigma_p(10^{-3})$
	First group	Second	Third	Average	
0°	1.456	2.194	2.462	2.037	7.971
5°	2.132	2.722	2.121	2.325	9.098
10°	2.413	2.763	2.474	2.55	9.978
15°	2.447	2.083	2.262	2.264	8.859
20°	2.954	2.980	2.93	2.955	11.56
25°	3.231	3.223	2.957	3.137	12.28
30°	3.243	3.378	3.15	3.257	12.75
35°	3.152	3.072	2.986	3.07	12.01
40°	3.391	4.433	3.395	3.74	14.64
45°	3.173	3.013	3.176	3.121	12.21
50°	4.343	3.755	4.431	4.176	16.34
55°	3.758	4.968	3.698	4.141	16.21
60°	6.045	7.733	5.955	6.578	25.75
65°	6.683	7.50	6.435	6.873	26.89
70°	8.521	8.236	8.325	8.361	32.72
75°	12.93	9.574	12.36	11.63	45.5

5.2. 3D Reconstruction Experiment

According to the above viewpoint planning and screening method, the viewpoint planning and reconstruction for the physical target.

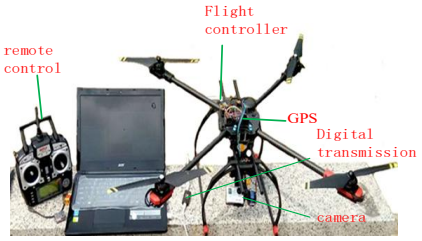

Figure 5. experiment system.

Figure 6. Planning viewpoint reconstruction results.

Figure 5 is an experimental system. The pose control software loads the planned waypoint file and transmits the waypoint command to the flight controller via the ground station using the wireless data transmitter. After receiving the command, the flight controller controls the drone and the camera to perform corresponding actions. When the planned specified viewpoint pose is reached, the pose control software sends a signal to trigger the camera to shoot. Cycle through the above process until all the waypoints are completed, and the shooting will automatically return to the landing.

The candidate viewpoint area is arranged, and the space arranged by the viewpoint is a hemisphere having a radius of a shooting distance (7.5 m). Using the latitude and longitude division method to obtain 500 candidate viewpoints, and then screening to obtain a set of 70 viewpoint sub-viewpoints, the final planning and reconstruction results are shown in figure 6 and table 2.

Table 2. Comparison of shooting effects.

	This paper	Traditional method
Number of viewpoints	70	70
Number of reconstructed feature points	212202	162320
Laser point cloud contrast deviation	7.08cm	7.92cm
Laser point cloud comparison standard deviation	55.57mm	62.05mm

Through the comparison of reconstruction results, the reconstruction method of the viewpoint layout proposed in this paper can be more complete and the reconstruction accuracy is higher.

6. Conclusion

In this paper, the viewpoint path planning problem of multi-view 3D reconstruction for aerial image is determined, and the parameters of camera pose control are determined. The experimental results show that the proposed method has high coverage and the reconstruction accuracy is less than 0.1%.

Acknowledgment

This work was supported by the Natural Science Research Project of West Anhui University (grant numbers WXZR201906), Key Teaching and Research Projects of West Anhui University (grant numbers wxxy2018020, wxxy2019065), National College Students Innovation and Entrepreneurship Training Program 2018 (grant numbers 201810376038).

References

[1] Cowan C K, Kovesi P D 1988 Automatic sensor placement from vision task requirements, *IEEE Transac. Pattern Anal. Mach. Intel.* **10(3)** 407-16.

[2] Satorres Martínez S, Gómez Ortega J, Gámez García J, Sánchez García A 2009 A sensor planning system for automated headlamp lens inspection, *Expert Syst. Appl.* **36** 8768-77.

[3] Abrams S, P. K. Allen, K. Tarabanis 1999 Computing Camera Viewpoints in an Active Robot Work-Cell, *Int. J. Robot. Res.* **18(3)**.

[4] W. R. Scott, G. Roth, View Planning for Automated Three-Dimensional Object Reconstruction and Inspection, ACM Comput. Surveys, **35(1)** 64-96.

[5] G. Olague 2000 Design and Simulation of Photogrammetric networks using Genetic algorithms, ASPRS 2000 Annual Conference Proceeding, Washington DC, USA.

[6] E. Dunn, G. Olague 2004 Milti-objective Sensor Planning for Efficient and Accurate Object Recinstruction, EvoWorkshops 2004, LNCS 3005, pp. 312-21.

[7] K. Schmid, H. Hirschmuller 2012 View Planning for Multi-View Stereo 3D Reconstruction Using an Autonomous Multicopter, *J. Intell. Robot. Syst.* **65** 309-23.

[8] X. zhen 2014 UAV aerial image-based three-dimensional reconstruction of outdoor scenes, Zhejiang University of Technology.

[9] G. Olague, R. Mohr 2002 Optimal camera placement for accurate reconstruction, Pattern Recongnition, **35(4)** 927-44.